Investigating the Spatial Variability in Soil Geochemical and Colour Properties Across Two Contrasting Land Uses

Maria Luna Miño[a], Alexander J Koiter[b,*], Taras E Lychuk[c], Arnie Waddel[c], Alan Moulin[c]

[a] *Brandon University, Masters in Environmental and Life Sciences, 270 18th St, Brandon, R7A 6A9*

[b] *Brandon University, Department of Geography and Environment, 270 18th St, Brandon, R7A 6A9*

[c] *Agriculture and Agri-Food Canada, Brandon Research and Development Centre, 2701 Grand Valley Road, Brandon, R7A 5Y3*

Abstract

Quantification and accurate assessment of the spatial variability and distribution of soil physical and biogeochemical properties are vital components of agri-environmental research and modeling, including sediment source fingerprinting. Understanding the distribution of soil properties is crucial in the development of appropriate, reliable, and efficient sampling campaigns. This study was aimed to investigate the spatial variability in soil geochemical and colour (i.e., spectral reflectance) soil properties (<63um) across two contrasting land uses. The main objectives of this study are to: 1) quantify the spatial variability of geochemical and colour properties at a field-scale (~ 40 ha) across agricultural and forested sites; 2) evaluate the spatial variability and distribution of soil properties and its relation to seven terrain attributes (e.g., catchment area, elevation). A combination of univariate analysis and geostatistical methods were applied to characterize the soil geochemistry and colour properties. This information was used to both quantify and assess the variability in soil properties. The variability and spatial autocorrelation were generally both site and soil property specific. For a selection of soil properties exhibiting some spatial autocorrelation, random forest regression was used to indentify the relative importance of terrain attributes on observed patterns of soil geochemical and colour properties. Elevation was found to explain the greatest amount of the variation in soil properties followed by the SAGA wetness index and relative slope position.

*Corresponding author

Email addresses: LUNAMIMA56@brandonu.ca (Maria Luna Miño), koitera@brandonu.ca (Alexander J Koiter), taras.lychuk@AGR.GC.CA (Taras E Lychuk), arnie.waddell@AGR.GC.CA (Arnie Waddel), apmaafc7788@gmail.com (Alan Moulin)

These types of information can be used to help create efficient soil sampling designs by providing information that can inform sampling locations and number of samples collected in order to meet research needs and objectives.

Keywords: Soil geochemistry, Soil colour, Spatial analysis

1. Introduction

Variation in soil biological, chemical, and physical properties occurs across the landscape and in response to both regional and local (i.e., field-scale) variations in the five soil forming factors: parent material, relief or topography, biota, climate, and time. Superimposed on this is the influence of changes in land use and current and historic management practices which can further modify soil properties. Quantifying and understanding the patterns and drivers for this variation is an important component of many agri-environmental studies. For example, to meet the desired level of precision for agronomic and environmental nutrient management plans the spatial variability in soil nutrients will influence the soil sampling design in terms of number and locations of soil samples [1, 2].

Sediment source fingerprinting is a watershed-scale technique that is used to identify and quantify the relative proportions of sediment derived from unique sources. This technique uses natural occurring biogeochemical properties as fingerprints (i.e., tracers) to discriminate between potential sources of sediment and are linked to downstream sediment using mixing models. From a sediment fingerprinting perspective, investigating the spatial variability of soil properties at a watershed-scale can be advantageous to identify, classify, and distinguish between potential sources of sediment [3]. However, investigating spatial variability at smaller scales is less common [e.g., 4, 5, 6, 7] and remains a research priority [8].

There are three main, interconnected, ways that spatial variability in fingerprint properties are an important aspect of sediment fingerprinting. First is to adequately quantify the fingerprint properties such that it is representative of that source. For some fingerprints the variability is not random but rather varies in a more systematic way. For example, the pattern of fallout radionuclides will reflect the patterns of soil erosion and deposition [9]. Designing and implementing source sampling plans need to take this into consideration as the sampling designed used has been shown to influence the characterization of wide range of commonly used fingerprints [7].

Secondly, the issue of spatial variability of fingerprint properties is further complicated by overlying spatial variability in the rates of erosion and sediment delivery. Incorporation of both types of variability into the mixing model will provide a more reliable estimate of the proportion of sediment derived from each source. Many mixing models have well defined inputs (sources) and outputs (sediment) that are characterized by their mean and standard deviation and the spatial distribution or pattern of fingerprints are not considered. This is not

ideal as the values of samples that are collected closer, and more hydrologically connected, to the stream network may in fact a better representation of that source despite potentially deviating from the mean value. This issue can be addressed by strategic sampling where the more likely to erode areas are targeted for sampling. However, a considerable amount of information and insight is lost through that approach. There has been some progress using information on erosion rates to calculate a erosion rate-weighted mean [9, 4] and using spatially interpolated maps of fingerprint values to provided a finer resolution of the fingerprint variability within each source [10].

Secondly, understanding the geomorphic, hydrologic, and biochemical processes that have led to the observed patterns in spatial variability helps in the selection of robust and reliable fingerprints and/or guide the sampling design for source characterization. In selecting fingerprints that provide good discrimination between sources many studies typically used a statistical-based approach [11]. However, there are concerns that this approach may result in the inclusion of false positives (i.e., type I error) or non-conservative fingerprints [12]. Consequently, there has been a call for the inclusion of a process-based (e.g., weathering, erosion) or geologic/lithologic-based explanation of the fingerprints selected to address these concerns [8]. Furthermore, there is also a lack of standardization in how sediment source areas are sampled (e.g., judgement, random, transect, grid, stratified) and it can be difficult to have an efficient sampling design without prior knowledge of why and how soil properties vary across the landscape [7]. Prior knowledge of the spatial variability of soil fingerprint properties would be beneficial; however, in practice this can be difficult, particularly with geochemical properties as routine lab analysis often return information on more than 50 elements. The spatial patterns of some soil properties are well studied because of their agronomic importance or ability to infer other important soil properties and processes and can include fallout radionuclides [e.g., ^{137}Cs, ^{7}Be; [13]], plant nutrients [e.g., N, P; [14]], soil colour [e.g., hue, value; [15]], major non-acid forming cations [e.g., Ca, Na; [16]]. In contrast, other soil properties including rare Earth elements and trace metals the processes leading to their distribution across the landscape is less studied or it is difficult to make generalizations (i.e., site specific).

Terrain attributes such as elevation, slope curvature, slope position, and soil wetness have been shown to be useful information in the understanding and modelling of a range of soil properties including soil moisture [17], texture [18], colour [19], organic matter [20], conductivity [21], and geochemistry [22]. Similar techniques may provide additional insight into the pedologic and geomorphic processes that drive the observed patterns of fingerprint properties within a given source. This information can be used to guide sampling design and interpret the data it provides.

This study builds on the previous work of Luna Miño [7] where the impact of three different sampling designs on the characterization of source materials, within the framework of the sediment fingerprinting approach, was assessed.

This study expands that study by using the data from grid sampling approach to assess the spatial autocorrelation, create iso-fingerprint maps, and identify important terrain attributes driving the observed patterns. The objectives of this study were (1) to investigate the spatial variability of a range of soil colour and geochemical properties in an agricultural and forested site; and (2) to assess the relative importance and correlation of terrain attributes with the spatial distribution of these soil properties.

2. Methods

2.1. Site description

Two sites of contrasting land uses located in the Wilson Creek Watershed (WCW), near McCreary, Manitoba, Canada were selected to investigate the spatial variability in fingerprint properties. The headwaters of the WCW are located on top of the Manitoba Escarpment within the boundary of Riding Mountain National Park. There is a ~300m drop in elevation crosses the escarpment where the streams become deeply incised. At the base of the escarpment is a large alluvial fan situated in the lacustrine deposits of glacial lake Aggasiz where the main stem has a meandering form. However, beyond the national park boundary the stream flows straight through an engineered drain until it reaches the Turtle river (Figure 1). Both sites are both hydrologicaly connected to the mainstem of the Wilson Creek

The first site was a mixedwood forest including white and black spruce (Picea glauca, Picea mariana), balsam fir (Abies balsamea), larch (Larix laricina) and young stands of deciduous trees including trembling aspen (Populus tremuloides). The forested site is located within the boundaries of the national park where there is little disturbance beyond recreational hiking trails. The soil within the park are not well mapped but likely are part of the Grey Wooded soil association (Luvisol) consisting of fine sandy loam to clay loam soils developed on boulder till of mostly shale with some limestone, and granitic rocks [23]. The second site is under agricultural production and includes rotations of grain crops and forage. The site is mapped to the Edwards Soil Series (Cumulic Regosol) consisting of silty clay loam to silty clay soil developed on recent alluvial deposits [23].

The Köppen-Geiger climate classification of the WCW is cold, without dry season, and with warm summer (Dfb) [24]. The average annual precipitation is ~539 mm, with approximately 27% falling as snow with a mean annual temperature is 3.0°C [25]. The hydrology of the watershed is snowmelt dominated with ~ 80% of the cumulative runoff occurring during the spring season (May and June) [26].

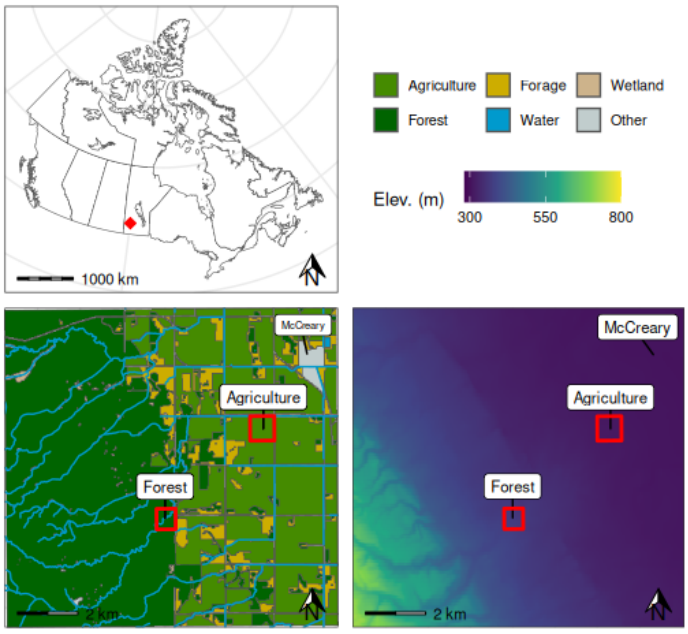

Figure 1: Map showing the location of the study sites within Canada, and the regional land use and topography.

Source: Research Site Locations

2.2. Soil sampling and analysis

This study uses samples and data collected as part of the grid sampling design outlined in Luna Miño [7]. Briefly, at each site 49 samples were collected using a soil auger on a 7x7 grid at a 100m spacing. Within the forested surface soil samples were collected below the LFH layer to a depth of 5cm, and the agricultural site was sampled to a depth of 15cm to account for the regular mixing of the soil due to tillage and other field operations.

Samples were dried, homogenized with a motar and pestle, and sieved through a 63 m sieve to remove the sand fraction. The sand fraction was removed in an effort to reduce the differences in grain size and organic matter content between the two sites [27]. Samples were analyzed for a broad suite geochemical element using inductively coupled plasma mass spectrometry (ICP-MS) following a microwave-assisted digestion with aqua-regia (ALS Mineral Division, North Vancouver, BC, Canada). Spectral measurements were made with a spectroradiometer (ASD FieldSpecPro Malvern Panalytical Inc Westborough MA 01581, United States). Spectral reflectance measurements were taken in 1 nm increments over the 0.4-2.5 m wavelength range. Both samples and Spectralon standard (white reference) were illuminated with a white light source using a

halogen-based lamp (12 VDC, 20 Watt). Following the method outlined in Boudreault et al. [28], fifteen colour coefficients (R, G, B, x, y, Y, X, Z, L, a*, b*, u*, v*, c*, h*) were calculated for each sample [29]. Based on the results of Luna Miño [7], a composite fingerprint consisting of 10 geochemical elements (Ca, Co, Cs, Fe, Li, La, Nb, Ni, Rb, and Sr) and five colour coefficients (a, b, c, h, and x) were identifying as providing a strong discrimination between the agricultural and forested surface soils. These fifteen soil properties are the focus of the detailed spatial analysis detailed in this study.

2.3. Geospatial and terrain analysis

All geostatistics were performed with ArcGIS Pro [v 3.3.0 30]. Semivariograms were used to quantify spatial correlation for each of the 15 soil properties. The optimization tool, based on minimizing the mean square error, was used to parameterize the semivariogram model. Kriging was used to interpolate and generate maps of each soil property. The exploratory interpolation tool (Geostatistical Analyst extension) was used to select the kriging type with the highest ranked prediction accuracy.

A Digital Elevation Model (DEM) for the forested site was acquired from publicly available data [31]. A DEM for the agricultural site was generated by photogrammetry using UAV imagery, including the use of ground control and check points, with Agisoft Metashape Professional [v1.8.2 32]. Ordinary kriging was used to calculate a 1 m gridded digital elevation model for each site. Geographic information software [SAGA v2.1.4 33] was used to calculate six additional terrain attributes and included plan and profile curvatures, saga wetness index, catchment area, relative slope position, vertical channel network distance.

2.4. Data analysis

All subsequent statistical analysis was undertaken using R statistical Software v4.4.0 [34] through RStudio Integrated Development Environment v2024.04.2 [35]. Plots and maps were created using the R package `ggplot2` v 3.5.2 [36]. Skewness was categorized as values between -0.5 and 0.5 considered approximately symmetric, -1.0 to -0.5 or 0.5 to 1 as moderately skewed, and $<$ -1.0 or $>$ 1.0 as highly skewed. Coefficient of variation (CV) thresholds were categorized as low (<15%), moderate (15–35%), high (35–75%), and very high (>75%) .Interpolated soil property and terrain attribute data were resampled to a 10 m resolution prior to analysis [`terra` v1.8.42 37]. Random Forest Regression [`randomForest` v4.7.1.2 38] was used to assess the relative importance of the terrain attributes on the spatial distribution of soil properties. The dataset was randomly split into training, validation, and testing datasets. Multicollinearity among the terrain attributed was assessed using the Variance Inflation Factor with a threshold of eight and correlated terrain attributes were removed [`usdm` v2.1.7 39]. The number of variables randomly sampled as candidates at each split within the random forest model was tuned using the training and validation data sets [`caret` v7.0.1 40]. The number of trees to grow was set to 500

and assessed using the Root Mean Square Error for both the Out of Bag Error and the validation data sets. To test the model, actual and predicted values were plotted and the R^2 was calculated.

3. Results

3.1. Univariate summary

Overall, the agricultural site had soil colour and geochemical properties that exhibited lower variability and more symmetrical data distributions as compared to the forested site. Considering all 15 colour properties measured it was observed that all the colour properties for both sites exhibit an approximate symmetric distribution. All 15 colour properties for the agriculture site had a low CV and the forested site had slightly greater variability with 10 colour properties the a low CV and five with a moderate CV. Overall, the agricultural site had lower variability and the distribution of data for each element were generally more symmetrical as compared to the forest site. Of the 44 geochemical concentrations measured at the agricultural site, nine elements exhibited moderately skewed distributions, while five displayed highly skewed distributions. Additionally, 12 elements had moderate coefficients of variation (CV), and five had high CV. At the forested site, seven elements showed moderately skewed distributions and 14 exhibited highly skewed distributions. Furthermore, 28 elements had moderate CV, six had high CV, and two had very high CV.

Table 1: Summary univariate statistics of selected geochemical and colour soil properties for each site (n = 49).

Property	Mean	SD	Max	Min	Skewness	CV
			Agriculture			
Ca	4.00	2.19	8.78	0.95	0.28	54.66
Co	8.76	0.83	10.60	7.50	0.52	9.48
Cs	0.75	0.15	1.07	0.47	0.18	19.93
Fe	1.92	0.09	2.11	1.71	−0.25	4.70
Li	15.62	1.42	19.80	12.80	0.62	9.11
La	18.23	1.22	20.20	15.50	−0.29	6.71
Nb	0.59	0.06	0.73	0.46	0.45	9.67
Ni	29.63	2.72	35.70	25.00	0.36	9.17
Rb	18.43	4.33	26.70	10.20	0.24	23.48
Sr	91.31	38.98	163.50	38.60	0.09	42.69
a*	3.38	0.32	4.15	2.59	−0.03	9.53
b*	8.84	0.97	10.59	6.69	−0.18	11.00
c*	9.47	1.02	11.32	7.17	−0.19	10.74
h*	1.20	0.01	1.23	1.18	0.19	1.12
x	0.47	0.00	0.48	0.47	0.06	0.46
			Forest			
Ca	1.89	1.53	5.46	0.47	1.07	81.12

Table 1: Summary univariate statistics of selected geochemical and colour soil properties for each site (n = 49).

Property	Mean	SD	Max	Min	Skewness	CV
Co	6.76	1.39	9.60	4.00	0.03	20.62
Cs	0.55	0.12	0.78	0.34	0.25	21.73
Fe	1.18	0.13	1.46	0.83	−0.58	11.24
Li	6.47	0.90	8.60	4.30	−0.02	13.89
La	15.00	2.60	21.80	10.30	0.33	17.31
Nb	0.37	0.06	0.56	0.17	−0.68	17.10
Ni	18.09	3.90	28.00	11.00	0.33	21.55
Rb	13.83	1.85	18.10	9.90	0.27	13.40
Sr	32.43	12.60	64.20	15.30	0.98	38.87
a*	5.73	0.41	6.56	4.41	−0.38	7.10
b*	12.47	2.01	15.91	8.02	0.22	16.11
c*	13.74	1.94	17.00	9.15	0.15	14.15
h*	1.13	0.05	1.23	1.06	0.34	4.13
x	0.49	0.00	0.49	0.48	−0.21	0.47

Source: Univariate summary

The agricultural site has a relatively flat topography with an elevation change of approximately 3m, with the field draining toward a ditch in the northeast corner. The forested site has a relatively more complex topography, with a channel flowing from the southwest toward the northeast and an overall elevation difference of 18 m across the site. The mean plan and profile curvature measurements for both sites are near zero indicating a area of sediment transit and not accumulation or erosion. The agricultural site had a higher SAGA Wetness Index but the forested site had a larger range in values and exhibited a higher degree of variability. The forested site exhibited a smaller mean Relative Slope Position value (streams and depressional areas) and a smaller Vertical Distance to Channel Network, and for both terrain attributes a greater variability as compared to the agricultural reflecting the presence of the stream crossing the forested site.

Table 2: Summary statistics for the interpoloated values (10m resolution) for slected geochemical and colour soil properties and terrain attributes for each site.

Property	Mean	SD	Max	Min	Skewness	C
			Agriculture			
Ca	4.12	2.10	8.76	0.918	0.0727	51
Co	8.75	0.664	10.6	7.52	0.431	7.
Cs	0.729	0.123	1.07	0.458	0.376	16
Fe	1.92	0.0644	2.10	1.73	−0.450	3.
Li	15.7	1.16	19.3	13.2	0.551	7.

Table 2: Summary statistics for the interpoloated values (10m resolution) for slected geochemical and colour soil properties and terrain attributes for each site.

Property	Mean	SD	Max	Min	Skewness	C
La	18.2	0.817	19.8	16.5	−0.268	4.
Nb	0.593	0.0550	0.740	0.459	0.569	9.
Ni	29.9	2.23	34.5	26.3	−0.0100	7.
Rb	18.0	3.94	26.1	11.5	0.498	2
Sr	93.4	38.6	167	36.3	0.00105	4
a*	3.34	0.211	3.83	2.88	0.0621	6.
b*	8.73	0.707	10.2	6.98	−0.162	8.
c*	9.34	0.762	11.0	7.41	−0.158	8.
h*	1.20	0.00977	1.23	1.18	−0.0603	0.
x	23.1	1.31	26.6	18.6	−0.501	5.
Plan Curvature	1.65×10^{-6}	1.36×10^{-4}	6.57×10^{-4}	-5.07×10^{-4}	3.54×10^{-1}	8.24
Profile Curvature	-7.64×10^{-6}	1.53×10^{-4}	5.83×10^{-4}	-6.47×10^{-4}	9.51×10^{-2}	−2.00
SAGA Wetness Index	9.64	0.704	11.2	7.77	−0.122	7.
Catchment Area	475	1,010	10,100	4.35	4.76	2
Rel. Slope Position	0.718	0.288	1.20	0.0221	−0.946	4
Vert. Dist. Channel	5.98×10^{-2}	4.10×10^{-2}	2.92×10^{-1}	4.25×10^{-3}	1.21	6.85
Elevation	310	0.593	312	309	0.615	0.
			Forest			
Ca	1.88	0.769	3.61	0.787	0.202	4
Co	6.80	0.632	8.66	4.93	−0.200	9.
Cs	0.551	0.0737	0.714	0.423	0.297	1
Li	6.43	0.694	8.46	4.39	−0.136	1
La	15.0	1.57	18.5	11.5	−0.0324	1
Nb	0.370	0.0356	0.440	0.278	−0.436	9.
Ni	18.2	2.49	24.9	14.3	0.314	1
Sr	31.6	8.50	53.1	18.1	0.716	2
h*	1.13	0.0371	1.22	1.06	0.257	3.
x	19.7	3.92	30.5	10.8	0.362	1
Plan Curvature	3.97×10^{-4}	3.27×10^{-3}	2.89×10^{-2}	-2.62×10^{-2}	7.91×10^{-1}	8.22
Profile Curvature	-1.83×10^{-4}	9.47×10^{-3}	6.37×10^{-2}	-7.37×10^{-2}	-5.31×10^{-1}	−5.18
SAGA Wetness Index	6.00	0.988	8.48	2.21	−0.430	1
Catchment Area	571	1,940	25,400	3.44	6.60	3
Rel. Slope Position	0.222	0.232	0.993	0.00617	1.56	1
Vert. Dist. Channel	4.15×10^{-1}	4.43×10^{-1}	3.66	2.02×10^{-2}	2.96	1.07
Elevation	369	3.34	377	359	−0.184	0.

Source: Univariate summary

3.2. Spatial analysis

Soil colour and geochemical composition varied across both sites. In the agricultural field, all 15 soil color and geochemical properties exhibited spatial au-

tocorrelation with most properties demonstrating a strong spatial dependency. Some of the soil properties presented a pattern that roughly matches (e.g., Rb, Cs) or mirrors (e.g., Ca, Sr) the overall topography of the site with a gradation between the highest point in the south-west corner towards the lowest points in the north-east. Other properties appear to have more localized highs and low concentrations/values (e.g., c*, h). The geochemical concentrations of Ca and Rb had the largest range values and as result displayed a less patchy distribution across the site. The nugget (Co) was small for all soil properties (<1.5), and Sr had an exceptionally large sill value (900).

At the forested site, the geochemical concentrations of Fe and Rb, along with the color properties a*, b*, c*, and x showed no spatial autocorrelation and were excluded from further analysis. Overall, the influence of the channel environment can be seen in the remaining nine soil properties. In comparison to the agricultural site, the soil properties at the forested site displayed a more moderate spatial dependency. The nugget (Co) was generally small for most soil properties (<2) with the exception of La and Ni. The range values were similar across the different soil properties and fell between 176 and 298 m.

Table 3: Geostatistical parameters of the fitted semivariogram models of selec
geochemical properties within the agricultural and forested sites.

Property	Kriging Type[1]	Nugget (Co)	Sill (Co + C)	C/(C + Co) (%)	Range (m)	r^2
					Agriculture	
Ca	Universal	0.0	7.2	100	580	0.9
Co	Simple	0.0	0.7	100	208	0.4
Cs	Ordinary	0.0	0.0	100	210	0.5
Fe	Ordinary	0.0	0.0	100	185	0.2
Li	Universal	0.3	1.5	81	185	0.6
La	Simple	0.4	1.0	56	308	0.5
Nb	Universal	0.0	0.0	91	210	0.7
Ni	Ordinary	1.4	8.9	84	352	0.6
Rb	Ordinary	1.4	27.6	95	551	0.9
Sr	Ordinary	0.9	900.2	100	220	1.0
a*	Ordinary	0.4	1.0	59	288	0.3
b*	Simple	0.2	0.9	83	199	0.3
c*	Simple	0.1	0.9	87	199	0.3
h*	Simple	0.0	1.1	100	185	0.2
x	Simple	0.4	1.0	58	220	0.1
					Forest	
Ca	Ordinary	1.6	2.7	41	269	0.2
Co	Ordinary	0.0	2.1	100	298	0.1
Cs	Ordinary	0.0	0.0	83	237	0.2
Li	Ordinary	0.0	0.8	100	222	0.3
La	Ordinary	3.1	7.4	59	176	0.1
Nb	Ordinary	0.0	0.0	51	224	0.2

Table 3: Geostatistical parameters of the fitted semivariogram models of selec
geochemical properties within the agricultural and forested sites.

Property	Kriging Type[1]	Nugget (Co)	Sill (Co + C)	C/(C + Co) (%)	Range (m)	r^2
Ni	Universal	6.7	15.8	57	187	0.2
Sr	Simple	0.4	1.0	65	229	0.4
h*	Universal	0.0	0.0	100	230	0.3
x	Ordinary	0.0	39.2	100	312	0.2

[1] Models are all isotropic.

[2] Strong spatial dependency (C/(C + Co) % >75); Moderate spatial dependency (C/(C + Co) % between 75

Source: Semivariograms

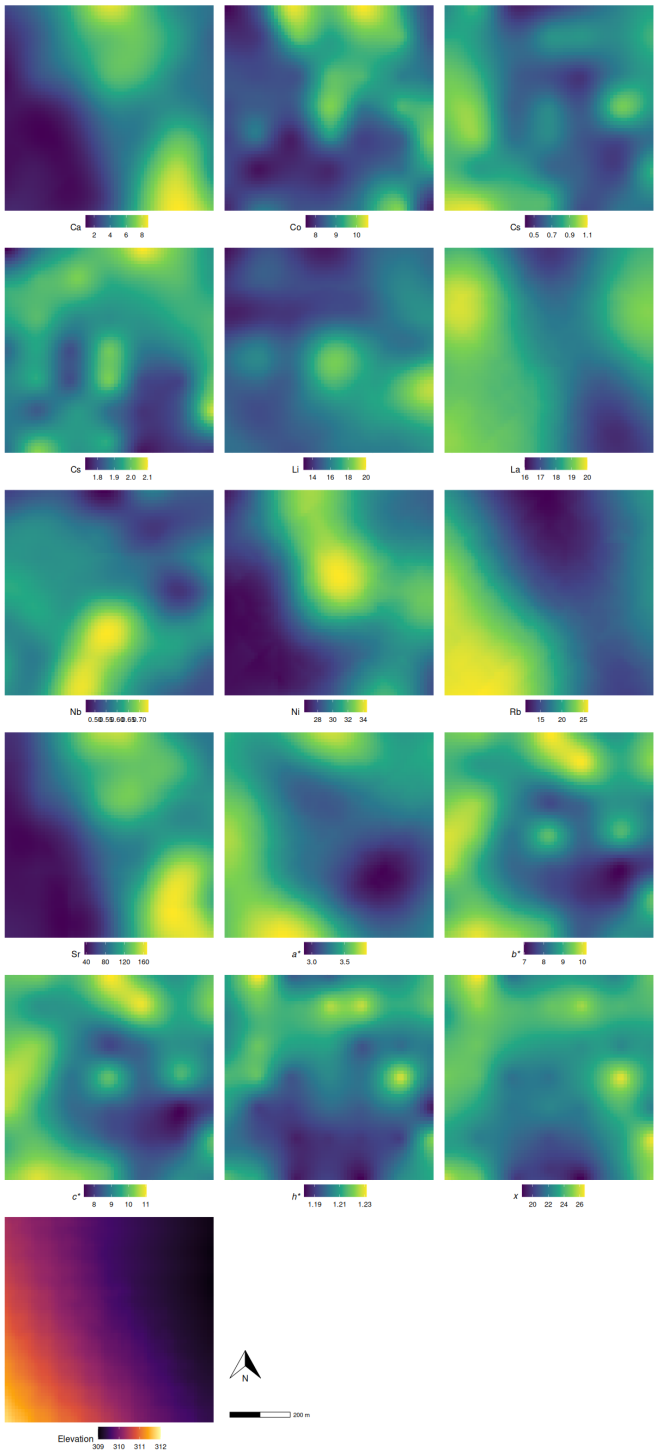

Figure 2: Kriged maps of select colour and geochemical properties and elevtion across the agricultural site.

Source: Soil property mapping

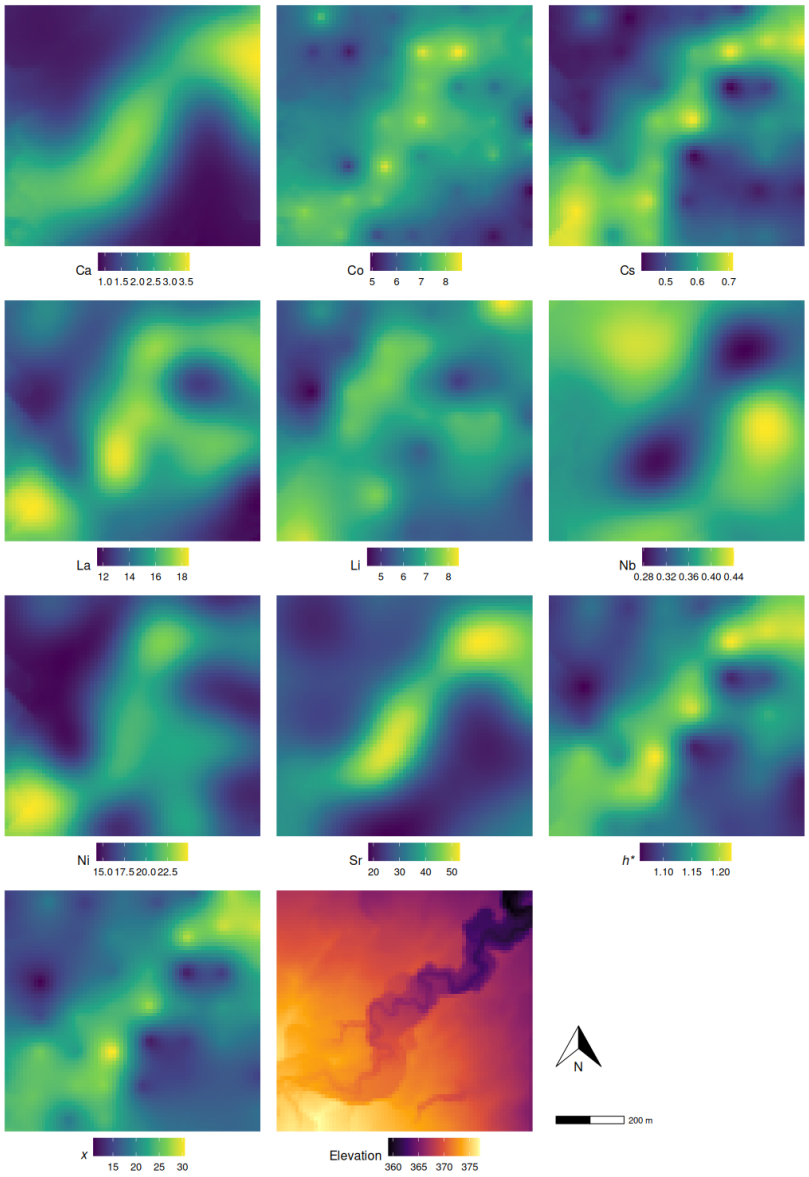

Figure 3: Kriged map of select colour and geochemical properties and elevation across the forested site.

Source: Soil property mapping

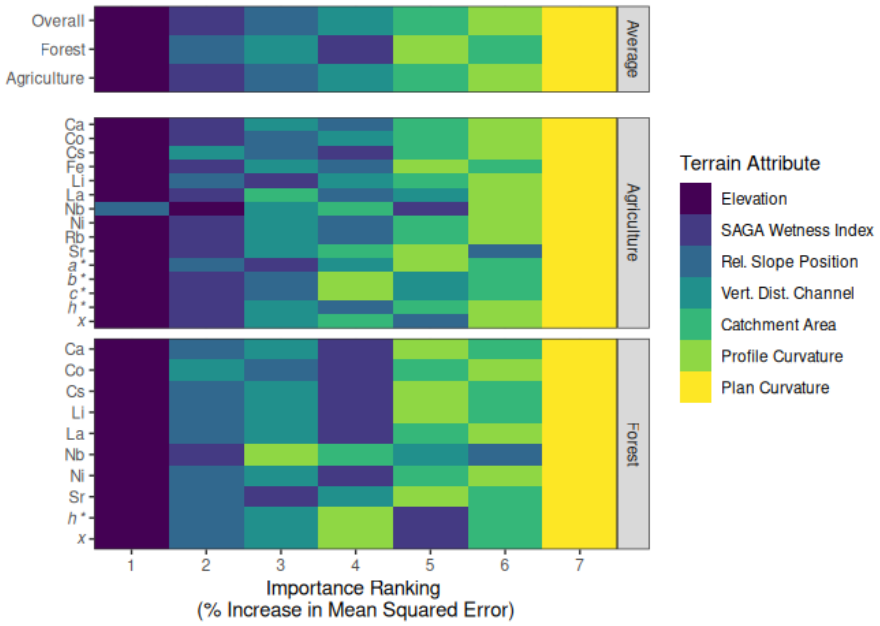

Figure 4: Heat map of the Random Forest regresssion results showing the ranking of the importance of terrain attributes (based on % increase in Mean Squared Error) in explaining the spatial variabilty of selected colour and geochemical properties within the agricultural and forested sites. Top panel shows an average ranking for each site and across both sites.

Source: Random Forest summary

Table 4: Model summary and performance statistics for the random forest regression using the training, validation, and test data sets.

Property	MSETraining[2]		MSETesting[1 2]		{{R^2}}Testing
			Agriculture		
Ca	0.374	91.6	0.359	91.8	0.91
Co	0.089	79.8	0.080	82.5	0.80
Cs	0.002	85.7	0.002	86.4	0.85
Fe	0.001	69.6	0.001	70.9	0.69
Li	0.538	59.3	0.533	59.8	0.64
La	0.048	93.0	0.044	93.1	0.93
Nb	0.001	57.3	0.001	59.1	0.55
Ni	0.338	93.1	0.335	93.7	0.93
Rb	0.733	95.3	0.643	96.1	0.95
Sr	97.221	93.5	93.970	93.6	0.93
a*	0.007	85.0	0.006	86.9	0.85
b*	0.136	72.5	0.120	75.3	0.72

Table 4: Model summary and performance statistics for the random forest regression using the training, validation, and test data sets.

Property	MSETraining[1]		MSETesting[1 2]		{{R^2}}Testing
c*	0.155	73.2	0.136	75.9	0.73
h*	0.000	58.3	0.000	58.6	0.56
x	0.628	61.9	0.701	61.8	0.59
			Forest		
Ca	0.231	61.1	0.231	60.7	0.63
Co	0.244	39.1	0.234	42.9	0.48
Cs	0.002	64.1	0.002	67.1	0.66
Li	0.278	41.3	0.282	42.0	0.46
La	1.401	43.3	1.323	47.5	0.48
Nb	0.001	55.0	0.001	55.9	0.58
Ni	2.819	55.2	2.806	56.0	0.55
Sr	29.427	59.4	29.663	59.1	0.59
h*	0.001	58.8	0.001	60.3	0.62
x	5.646	62.6	5.810	63.4	0.64

[1] Mean square error
[2] Percent variance explained

Source: Random Forest summary

4. Discussion

A large sill in a semivariogram indicates that the total variance of a soil property is high.

A soil property with a large range relative to other properties in a semivariogram indicates that spatial correlation persists over a greater distance. The property is relatively uniform over large areas, with gradual changes rather than abrupt variations.

References

[1] J. L. Starr, J. J. Meisinger, T. B. Parkin, Influence of sample size on chemical and physical soil measurements, Soil Science Society of America Journal 59 (3) (1995) 713–719, _eprint: https://acsess.onlinelibrary.wiley.com/doi/pdf/10.2136/sssaj1995.03615995005900030012x. doi:10.2136/sssaj1995.03615995005900030012x.
URL https://onlinelibrary.wiley.com/doi/abs/10.2136/sssaj1995.03615995005900030012x

[2] S. K. Kariuki, H. Zhang, J. L. Schroder, T. Hanks, M. Payton, T. Morris, Spatial variability and soil sampling in a grazed pasture, Communications

in Soil Science and Plant Analysis 40 (9-10) (2009) 1674–1687.
URL http://www.tandfonline.com/doi/abs/10.1080/00103620902832089

[3] S. Pulley, I. Foster, A. L. Collins, The impact of catchment source group classification on the accuracy of sediment fingerprinting outputs, Journal of Environmental Management 194 (2017) 16–26.
URL http://www.sciencedirect.com/science/article/pii/S0301479716302195

[4] P. Du, D. E. Walling, Fingerprinting surficial sediment sources: Exploring some potential problems associated with the spatial variability of source material properties, Journal of Environmental Management 194 (1) (2017) 4–15. doi:https://doi.org/10.1016/j.jenvman.2016.05.066.
URL http://www.sciencedirect.com/science/article/pii/S0301479716303218

[5] S. Pulley, A. L. Collins, B. Van der Waal, Variability in the mineral magnetic properties of soils and sediments within a single field in the cape fold mountains, south africa: Implications for sediment source tracing, CATENA 163 (2018) 172–183. doi:10.1016/j.catena.2017.12.019.
URL https://www.sciencedirect.com/science/article/pii/S0341816217304216

[6] A. L. Collins, E. Burak, P. Harris, S. Pulley, L. Cardenas, Q. Tang, Field scale temporal and spatial variability of 13c, 15n, tc and tn soil properties: Implications for sediment source tracing, Geoderma 333 (2019) 108–122. doi:10.1016/j.geoderma.2018.07.019.
URL https://www.sciencedirect.com/science/article/pii/S0016706118303185

[7] M. A. Luna Miño, A. J. Koiter, D. A. Lobb, Effect of sampling design on characterizing surface soil fingerprinting properties, Journal of Soils and Sediments 24 (5) (2024) 2180–2198. doi:10.1007/s11368-024-03805-x.
URL https://doi.org/10.1007/s11368-024-03805-x

[8] A. L. Collins, M. Blackwell, P. Boeckx, C.-A. Chivers, M. Emelko, O. Evrard, I. Foster, A. Gellis, H. Gholami, S. Granger, P. Harris, A. J. Horowitz, J. P. Laceby, N. Martinez-Carreras, J. Minella, L. Mol, K. Nosrati, S. Pulley, U. Silins, Y. J. da Silva, M. Stone, T. Tiecher, H. R. Upadhayay, Y. Zhang, Sediment source fingerprinting: benchmarking recent outputs, remaining challenges and emerging themes, Journal of Soils and Sediments 20 (12) (2020) 4160–4193. doi:10.1007/s11368-020-02755-4.
URL https://doi.org/10.1007/s11368-020-02755-4

[9] S. N. Wilkinson, J. M. Olley, T. Furuichi, J. Burton, A. E. Kinsey-Henderson, Sediment source tracing with stratified sampling and weightings based on spatial gradients in soil erosion, Journal of Soils and Sediments 15 (10) (2015) 2038–2051. doi:10.1007/s11368-015-1134-2.

URL http://proxy.library.unbc.ca:2118/article/10.1007/s11368-015-1134-2

[10] A. Haddadchi, M. Hicks, J. M. Olley, S. Singh, M. Srinivasan, Grid-based sediment tracing approach to determine sediment sources, Land Degradation and Development 30 (17) (2019) 2088–2106, _eprint: https://onlinelibrary.wiley.com/doi/pdf/10.1002/ldr.3407. doi:10.1002/ldr.3407.
URL https://onlinelibrary.wiley.com/doi/abs/10.1002/ldr.3407

[11] A. L. Collins, D. E. Walling, G. Leeks, Source type ascription for fluvial suspended sediment based on a quantitative composite fingerprinting technique, Catena 29 (1) (1997) 1–27. doi:https://doi.org/10.1016/S0341-8162(96)00064-1.
URL http://www.sciencedirect.com/science/article/B6VCG-3SVY7CV-1/2/17d8e824e1b6c26e15fcd31608eb6d05

[12] A. Koiter, P. Owens, E. Petticrew, D. Lobb, The behavioural characteristics of sediment properties and their implications for sediment fingerprinting as an approach for identifying sediment sources in river basins, Earth-Science Reviews 125 (2013) 24–42. doi:https://doi.org/10.1016/j.earscirev.2013.05.009.
URL http://www.sciencedirect.com/science/article/pii/S0012825213001074

[13] J. C. Ritchie, E. E. C. Clebsch, W. K. Rudolph, Distribution of fallout and natural gamma radionuclides in litter, humus and surface mineral soil layers under natural vegetation in the great smoky mountains, north carolina-tennessee, Health Physics 18 (5) (1970) 479.
URL https://journals.lww.com/health-physics/Abstract/1970/05000/Distribution_of_Fallout_and_Natural_Gamma.3.aspx

[14] D. Vasu, S. K. Singh, N. Sahu, P. Tiwary, P. Chandran, V. P. Duraisami, V. Ramamurthy, M. Lalitha, B. Kalaiselvi, Assessment of spatial variability of soil properties using geospatial techniques for farm level nutrient management, Soil and Tillage Research 169 (2017) 25–34. doi:10.1016/j.still.2017.01.006.
URL https://www.sciencedirect.com/science/article/pii/S0167198717300065

[15] R. A. Viscarra Rossel, B. Minasny, P. Roudier, A. B. McBratney, Colour space models for soil science, Geoderma 133 (3) (2006) 320–337.

[16] Y. Sun, W. Guo, D. C. Weindorf, F. Sun, S. Deb, G. Cao, J. Neupane, Z. Lin, A. Raihan, Field-scale spatial variability of soil calcium in a semi-arid region: Implications for soil erosion and site-specific management, PEDOSPHERE 31 (5) (2021) 705–714, num Pages: 10 Place: Beijing Publisher: Science Press Web of Science ID: WOS:000671191300005.

doi:10.1016/S1002-0160(21)60019-X.
URL https://www.webofscience.com/wos/woscc/summary/a5c79ace-f964-4a0b-90b2-d726580a394c-fae59ae2/relevance/1

[17] D. E. Beaudette, R. A. Dahlgren, A. T. O'Geen, Terrain-shape indices for modeling soil moisture dynamics, Soil Science Society of America Journal 77 (5) (2013) 1696–1710, _eprint: https://acsess.onlinelibrary.wiley.com/doi/pdf/10.2136/sssaj2013.02.0048. doi:10.2136/sssaj2013.02.0048.
URL https://onlinelibrary.wiley.com/doi/abs/10.2136/sssaj2013.02.0048

[18] V. Kokulan, O. Akinremi, A. P. Moulin, D. Kumaragamage, Importance of terrain attributes in relation to the spatial distribution of soil properties at the micro scale: a case study, Canadian Journal of Soil Science 98 (2) (2018) 292–305, publisher: NRC Research Press. doi:10.1139/cjss-2017-0128.
URL https://cdnsciencepub.com/doi/10.1139/cjss-2017-0128

[19] D. J. Brown, M. K. Clayton, K. McSweeney, Potential terrain controls on soil color, texture contrast and grain-size deposition for the original catena landscape in uganda, Geoderma 122 (1) (2004) 51–72. doi:10.1016/j.geoderma.2003.12.004.
URL https://www.sciencedirect.com/science/article/pii/S0016706104000035

[20] S. Zhang, Y. Huang, C. Shen, H. Ye, Y. Du, Spatial prediction of soil organic matter using terrain indices and categorical variables as auxiliary information, Geoderma 171-172 (2012) 35–43. doi:10.1016/j.geoderma.2011.07.012.
URL https://www.sciencedirect.com/science/article/pii/S001670611100214X

[21] B. P. Umali, D. P. Oliver, S. Forrester, D. J. Chittleborough, J. L. Hutson, R. S. Kookana, B. Ostendorf, The effect of terrain and management on the spatial variability of soil properties in an apple orchard, CATENA 93 (2012) 38–48. doi:10.1016/j.catena.2012.01.010.
URL https://www.sciencedirect.com/science/article/pii/S0341816212000136

[22] F. R. D. Lima, P. Pereira, I. C. F. Vasques, E. C. Silva Junior, M. Mancini, J. R. Oliveira, M. T. A. Prianti, C. Windmöller, D. C. Weindorf, N. Curi, B. T. Ribeiro, J. Richardson, J. Marques, L. R. G. Guilherme, Predictive modeling of total hg background concentration in soils of the amazon rainforest biome with support of proximal sensors and auxiliary variables, Journal of South American Earth Sciences 129 (2023) 104510. doi:10.1016/j.jsames.2023.104510.
URL https://www.sciencedirect.com/science/article/pii/S0895981123003218

[23] W. Ehrlich, L. Pratt, F. Leclaire, Reconnaissance soil survey of west-lake map sheet area, Tech. rep. (1958).

[24] H. E. Beck, N. E. Zimmermann, T. R. McVicar, N. Vergopolan, A. Berg, E. F. Wood, Present and future köppen-geiger climate classification maps at 1-km resolution, Scientific Data 5 (1) (2018) 180214, number: 1 Publisher: Nature Publishing Group. doi:10.1038/sdata.2018.214.
URL https://www.nature.com/articles/sdata2018214

[25] Environment, C. C. Canada, Canadian climate normals, meteorology, Weather (2024).
URL https://climate.weather.gc.ca/climate_normals/index_e.html

[26] G. MacKay, A quantitative study of geomorphology of the wilson creek watershed, manitoba, Ph.D. thesis, Winnipeg, MB, m.Sc., Civil Engineering (1970).

[27] J. P. Laceby, O. Evrard, H. G. Smith, W. H. Blake, J. M. Olley, J. P. G. Minella, P. N. Owens, The challenges and opportunities of addressing particle size effects in sediment source fingerprinting: A review, Earth-Science Reviews 169 (2017) 85–103. doi:https://doi.org/10.1016/j.earscirev.2017.04.009.
URL http://proxy.library.unbc.ca:2111/science/article/pii/S0012825216304548

[28] M. Boudreault, A. J. Koiter, D. A. Lobb, P. N. Owens, K. Liu, G. Benoy, S. Danielescu, S. Li, Using colour, shape and radionuclide sediment fingerprints to identify sources of sediment in an agricultural watershed in atlantic canada, Canadian Water Resources Journal 43 (3) (2018) 347–365. doi:https://doi.org/10.1080/07011784.2018.1451781.

[29] A. Koiter, Colour analysis scriptsDOI: 10.5281/zenodo.5123327 (07 2021). doi:10.5281/zenodo.5123327.
URL https://github.com/alex-koiter/Colour-analysis

[30] Esri, ArcGIS Pro, Esri, 2024.
URL https://www.esri.ca/

[31] N. R. Canada, High resolution digital elevation model mosaic (hrdem mosaic) - canelevation series (2024).
URL https://open.canada.ca/data/en/dataset/0fe65119-e96e-4a57-8bfe-9d9245fba06b

[32] Agisoft, Agisoft metashape: Installer (2021).
URL https://www.agisoft.com/downloads/installer/

[33] O. Conrad, B. Bechtel, M. Bock, H. Dietrich, E. Fischer, L. Gerlitz, J. Wehberg, V. Wichmann, J. Böhner, System for automated geoscientific analyses (saga) v. 2.1.4, Geoscientific Model Development 8 (7) (2015) 1991–2007, publisher: Copernicus GmbH. doi:10.5194/gmd-8-1991-2015.
URL https://gmd.copernicus.org/articles/8/1991/2015/

[34] R. C. Team, R: A language and environment for statistical computing (2024).
URL http://www.R-project.org

[35] RStudio, Rstudio: Integrated development environment for r (2024).
URL http://www.rstudio.org/

[36] H. Wickham, ggplot2: Elegant Graphics for Data Analysis, Springer-Verlag, New York NY U.S.A, 2016.

[37] R. J. Hijmans, terra: Spatial Data Analysis, r package version 1.7-78 (2024).
URL https://CRAN.R-project.org/package=terra

[38] A. Liaw, M. Wiener, Classification and regression by randomforest, R News 2 (3) (2002) 18–22.
URL https://CRAN.R-project.org/doc/Rnews/

[39] B. Naimi, N. a.s. Hamm, T. A. Groen, A. K. Skidmore, A. G. Toxopeus, Where is positional uncertainty a problem for species distribution modelling, Ecography 37 (2014) 191–203. doi:10.1111/j.1600-0587.2013.00205.x.

[40] Kuhn, Max, Building predictive models in r using the caret package, Journal of Statistical Software 28 (5) (2008) 1–26. doi:10.18637/jss.v028.i05.
URL https://www.jstatsoft.org/index.php/jss/article/view/v028i05

Supplemental figures

Supplemental tables

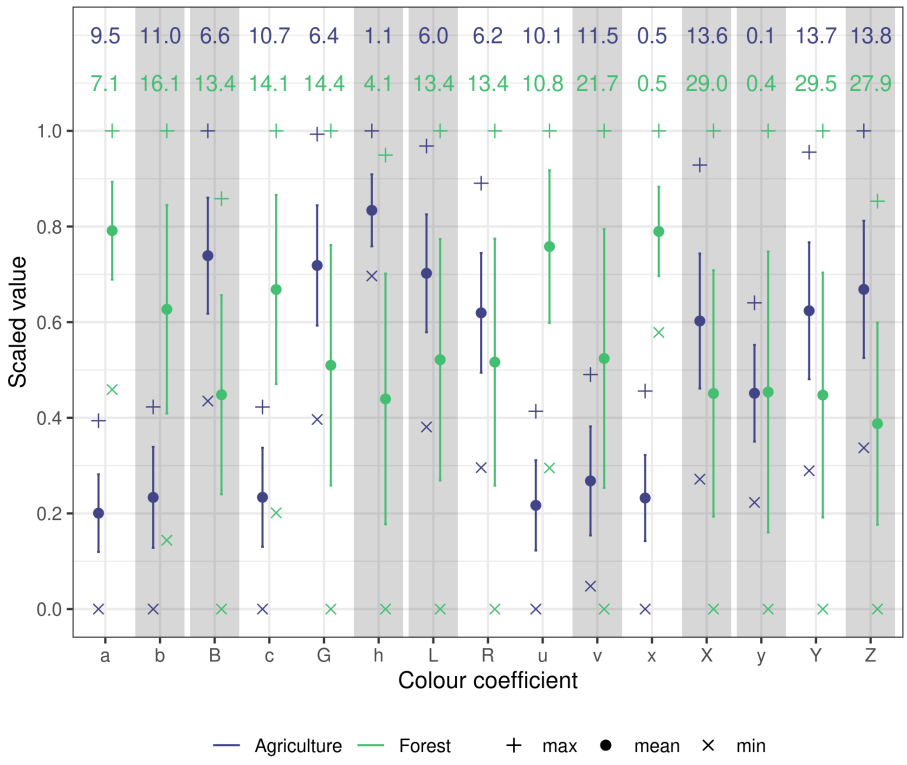

Figure S1: Summary statistics of all measured colour soil properties at both sites. Error bars represent 1SD and the numeric values indicate the CV.

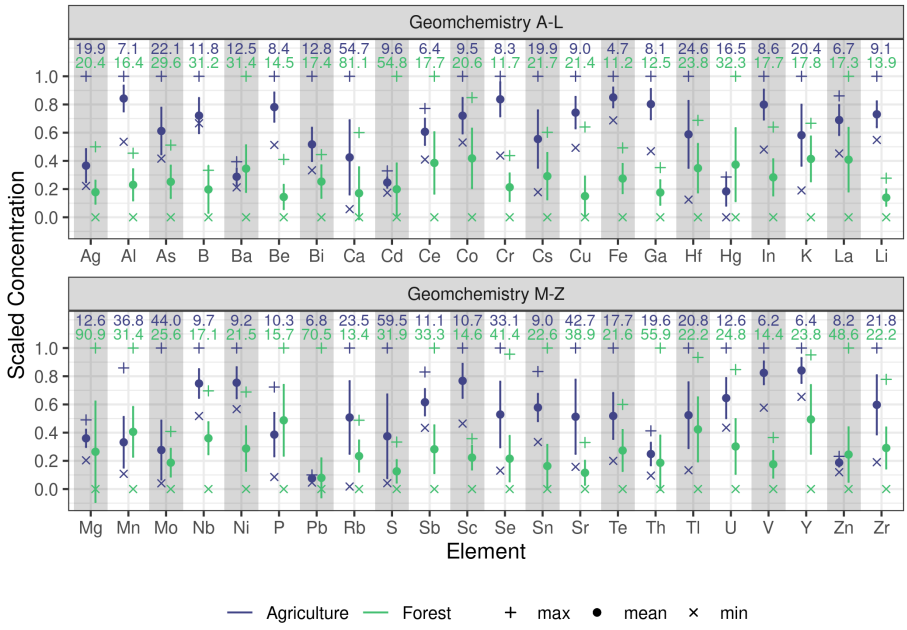

Figure S2: Summary statistics of all measured geochemical soil properties at both sites. Error bars represent 1SD and the numeric values indicate the CV.

Colour space model	Parameter	Abbreviation
RGB	Red	R
RGB	Green	G
RGB	Blue	B
CIE xyY	Chromatic Coordinate x	x
CIE xyY	Chromatic Coordinate y	y
CIE xyY	Brightness	Y
CIE XYZ	Virtual component X	X
CIE XYZ	Virtual component Z	Z
CIE LAB	Metric lightness function	L
CIE LAB	Chromatic coordinate opponent red–green scales	$a*$
CIE LAB	Chromatic coordinate opponent red–green scales	$b*$
CIE LUV	Chromatic coordinate opponent blue–yellow scales	$u*$
CIE LUV	Chromatic oordinate opponent red–green scales	$v*$
CIE LCH	CIE hue	$c*$
CIE LCH	CIE chroma	$h*$

Table S1: Description of spectral reflectance colour coefficients used as fingerprints. Reproduced from Boudreault et al. (2018)